Mechanism of Transcriptional Bursting in Bacteria

Cell

Mechanism of Transcriptional Bursting in Bacteria

Shasha Chong,[1,5] Chongyi Chen,[1,2,5] Hao Ge,[3,4] and X. Sunney Xie[1,3,*]
[1]Department of Chemistry and Chemical Biology, Harvard University, Cambridge, MA 02138, USA
[2]Department of Molecular and Cellular Biology, Harvard University, Cambridge, MA 02138, USA
[3]Biodynamic Optical Imaging Center (BIOPIC), Peking University, Beijing 100871, China
[4]Beijing International Center for Mathematical Research (BICMR), Peking University, Beijing 100871, China
[5]Co-first author
*Correspondence: xie@chemistry.harvard.edu
http://dx.doi.org/10.1016/j.cell.2014.05.038

SUMMARY

Transcription of highly expressed genes has been shown to occur in stochastic bursts. But the origin of such ubiquitous phenomenon has not been understood. Here, we present the mechanism in bacteria. We developed a high-throughput, in vitro, single-molecule assay to follow transcription on individual DNA templates in real time. We showed that positive supercoiling buildup on a DNA segment by transcription slows down transcription elongation and eventually stops transcription initiation. Transcription can be resumed upon gyrase binding to the DNA segment. Furthermore, using single-cell mRNA counting fluorescence in situ hybridization (FISH), we found that duty cycles of transcriptional bursting depend on the intracellular gyrase concentration. Together, these findings prove that transcriptional bursting of highly expressed genes in bacteria is primarily caused by reversible gyrase dissociation from and rebinding to a DNA segment, changing the supercoiling level of the segment.

INTRODUCTION

Essential for all cell functions, transcription, the synthesis of mRNAs from DNA carried out by RNA polymerase (RNApol), is the first step in gene expression. Many recent experiments have shown the general phenomenon that transcription of highly expressed genes occurs in stochastic bursts in bacteria (Golding et al., 2005; So et al., 2011; Taniguchi et al., 2010; Zong et al., 2010) and eukaryotic cells (Suter et al., 2011). A major source of gene expression noise, transcriptional bursting results in cellular diversity of an isogenic population, possibly enhancing survival of the population in the face of environmental uncertainty (Kussell and Leibler, 2005; Thattai and van Oudenaarden, 2004; Wolf et al., 2005). Golding and coworkers directly observed transcriptional bursting in real time by using MS2 loops to monitor mRNA production in *E. coli* (Golding et al., 2005). Our group reported a high-throughput, single-molecule fluorescence in situ hybridization (FISH) assay to measure the cellular copy number distribution of a particular mRNA for a large population of isogenic *E. coli* cells (Taniguchi et al., 2010). When mRNAs are generated with a constant flux, one expects a Poisson distribution of mRNAs across the population. Bursting transcription would lead to non-Poissonian distributions. For all the highly expressed *E. coli* genes, we found that the distributions are not Poissonian, with the Fano factor (variance divided by the mean of a given distribution) larger than one. This indicates the ubiquity of transcriptional bursting in bacteria.

However, the origin of bacterial transcriptional bursting is still unknown. Its stochasticity implies it is a single-molecule behavior: there is only one copy of the gene in the cell. Its universality implies that it cannot be attributed to a specific gene or protein factor. Rather, it must originate from a fundamental and general mechanism pertinent to the chromosomal DNA structure and its influence on transcription regulation.

It has been shown that *E. coli* chromosomal DNA is segregated to ~400 topologically constrained loops with an average size of 10,000 base pairs (Hardy and Cozzarelli, 2005; Postow et al., 2004). Recent work discussed that *E. coli* nucleoid-associated proteins such as H-NS and Fis can cause formation of DNA loops based on both chromosome conformation capture and superresolution optical imaging experiments (Wang et al., 2011). Such chromosome structure provides us a clue to explain the transcriptional bursting phenomenon (Figure 1). In such a DNA loop, transcription generates positive supercoiling ahead of the RNApol and negative supercoiling behind the RNApol (Deng et al., 2004; Liu and Wang, 1987; Samul and Leng, 2007; Tsao et al., 1989; Wu et al., 1988). There exist two major topoisomerases in *E. coli* cells, gyrase and topoisomerase I (Topo I), which release positive and negative supercoiling, respectively (Drlica, 1992). It is known that negative supercoiling formed during transcription elongation is rapidly removed by Topo I (Cheng et al., 2003). This is necessary because accumulation of negative supercoiling could lead to the formation of detrimental R loops, an RNA-DNA hybrid (Drolet, 2006). The activity of gyrase, on the other hand, is not as sufficient to keep up with transcription (Guptasarma, 1996), leading to positive supercoiling accumulation on the DNA loops containing highly transcribed operons (El Hanafi and Bossi, 2000).

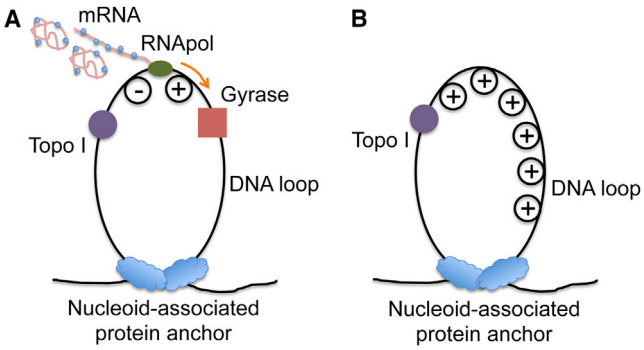

Figure 1. Transcription on Topologically Isolated Chromosomal DNA Loops

(A) Gyrase releases positive supercoiling generated by transcription on a DNA loop, and RNApol keeps transcribing the gene.

(B) In the absence of gyrase, active transcription on a DNA loop leads to positive supercoiling accumulation, which inhibits further transcription on the particular DNA loop.

It has been found that there are ~500 gyrase molecules per *E. coli* cell (Baker et al., 1987; Higgins et al., 1978; Liu and Wang, 1987), which happens to be roughly the number of topologically constrained DNA loops per chromosome. On average, there is one gyrase molecule per DNA loop. When a gyrase molecule reacts on the DNA loop, positive supercoiling is released, and RNApol can keep transcribing the gene ("on" state; Figure 1A). When the gyrase dissociates from the loop, positive supercoiling is built up by transcription, possibly slowing down transcription elongation and stopping transcription initiation ("off" state; Figure 1B).

In this study, through a series of in vitro single-molecule and live-cell experiments, we prove that transcriptional bursting of highly expressed genes in bacteria is primarily caused by gyrase dissociation from and reversible binding to a DNA segment or a chromosomal loop, which changes the supercoiling level of the DNA segment.

RESULTS

An In Vitro, Single-Molecule Assay Allows Real-Time Monitoring of Transcription on Individual DNA Templates

We developed an in vitro, single-molecule assay to monitor repetitive stochastic transcription events in real time on individual DNA templates with controlled supercoiling levels (Figure 2A). We used a nucleic acid stain, SYTO RNASelect (Life Technologies), which is nonfluorescent at 530 nm but becomes fluorescent upon binding to RNA (Figure 2B). It has been used to detect RNA in the presence of DNA (Kannemeier et al., 2007). An argon laser line at 488 nm was used to excite SYTO RNASelect in a total internal reflection fluorescence (TIRF) microscope. We collected fluorescence at 530 nm and recorded time-lapse movies with a charge-coupled device (CCD) camera. In the presence of the dye, a single nascent mRNA becomes visible, and its fluorescence intensity increases with the mRNA length. Therefore, we were able to track transcription elongation in real time as the nascent mRNA being produced on a surface-tethered DNA template. Transcription activities on up to hundreds of templates in one field of view can be monitored simultaneously.

As a control, we examined the effect of SYTO RNASelect on the activities of enzymes involved in our system, including T7 RNApol, *E. coli* RNApol, *E. coli* gyrase, and *E. coli* Topo I. None of them were found to be affected by the stain (Figures S1A–S1H available online). With sufficiently low laser power and the presence of a fresh oxygen scavenger system, photobleaching of the dye and photocleavage of nucleic acids were negligible (Figure S2).

In our single-molecule assay, DNA templates containing a promoter were tethered on the passivated surface of the flow cell through biotin-streptavidin linkage. After we flowed RNApol and nucleoside triphosphates (NTPs) into the flow cell, the fluorescence intensity of many spots in the field of view linearly ramped up due to transcription elongation, followed by abrupt disappearance upon transcription termination (Figure 2C). "Blinking" of fluorescence occurred when multiple transcripts were produced. As a control, no fluorescence intensity increase was observed under any of the following conditions: (1) no RNApol in the solution, (2) no NTPs in the solution, and (3) no promoter in the DNA template. Full-length transcripts (>12 kb) were generated as confirmed by RNA gel electrophoresis (Figures S1G–S1I).

By recording fluorescent movies, we were able to measure intensity versus time for a field of view containing hundreds of individual DNA templates, from which we could monitor how individual transcripts were generated (Figure 2D). This in vitro, single-molecule assay allows us to investigate the effects of supercoiling on transcription initiation and elongation in a clean and controlled system.

Positive Supercoiling Buildup by Transcription Slows Down Transcription Elongation

We examined the effect of positive supercoiling buildup on transcription elongation in vitro. We designed 12-kb-long linear DNA templates with T7 or *E. coli* promoter on the 5′ end and single or multiple biotinylated nucleotides on the 3′ end (Figure 3A).

When the DNA duplex is tethered to the surface with a single biotin-streptavidin linkage, we found the average T7 transcription elongation rate is 53.2 ± 3.4 nt/s (0.3 mM each NTP; 23°C), which is consistent with previously reported rates (Skinner et al., 2004). This result further proved that transcription was not affected by the SYTO RNASelect dye. In this case, supercoiling cannot accumulate because DNA can rotate around its single linkage to the surface.

On the other hand, DNA with multiple biotinylated nucleotides cannot rotate around its multiple linkages to the surface. Positive supercoiling would accumulate downstream of the elongation complex when spiral of the bulky complex around the DNA is hindered by the frictional drag on the complex. Interestingly, we found T7 transcription elongation was slowed down by 38% as positive supercoiling accumulated on the multiple-biotin DNA template (Figure 3B).

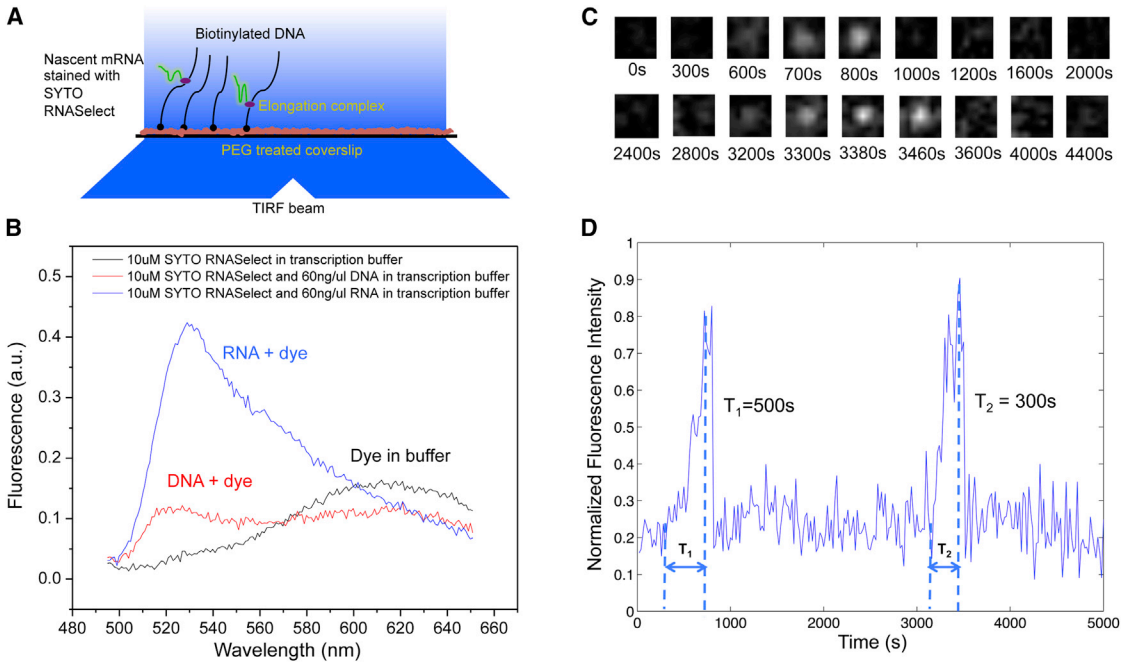

Figure 2. In Vitro, Single-Molecule Assay to Monitor Real-Time Transcription on Individual DNA Templates Using SYTO RNASelect Stain

(A) Schematic representation of the experimental arrangement (not drawn to scale). In the presence of 250 nM SYTO RNASelect, nascent RNAs are fluorescent under TIRF excitation at 488 nm. With an excitation power density of 0.22 W/cm^2 and an image acquisition time of 5 s, a transcript of 2,300 nucleotides yields a signal-to-noise ratio of 1.

(B) Fluorescence emission spectra of SYTO RNASelect solution under 488 nm excitation. The dye selectively stains RNA and emits fluorescence with a peak at 530 nm. In the absence of nucleic acids, the dye is not fluorescent at 530 nm. a.u., arbitrary units.

(C) Time-lapse images of 1.1 × 1.1 μm sub-field of view to monitor T7 transcription on one 12-kb-long template.

(D) Intensity-versus-time trajectory of the DNA template shown in (C). Full transcripts are produced repetitively on the template, with transcription elongation time T_1 = 500 s and T_2 = 300 s, respectively.

See also Figures S1 and S2.

There is a concern that supercoiling might arise from immobilization of the elongation complex to the surface. Special care was taken to minimize interactions of the elongation complex with the surface in our experiment. Besides, we note our result is consistent with the earlier in vitro report that the frictional drag on a sizable nascent transcript is enough to lead to DNA supercoiling (Tsao et al., 1989) even in aqueous solution and free of surface perturbation. Moreover, the measured elongation rate with the single linkage did not seem to be perturbed by the surface interaction with the elongation complex, if any.

Interestingly, the elongation rate on the multiple-biotin template was recovered when gyrase was added into the system. Figure 3C shows the elongation rate as a function of gyrase concentration, reaching the value of the single-biotin template at a saturating gyrase concentration. As a control, we found that gyrase did not affect the elongation rate on the single-biotin template (Figure 3C), indicating that gyrase play no other role than releasing positive supercoiling.

Similarly, with *E. coli* RNApol, we found positive supercoiling accumulation on the multiple-biotin template also slowed down transcription elongation by 47% (Figure 3D), which is consistent with a recent report based on mechanical manipulation (Ma et al., 2013).

Dissociation Constant of Gyrase-DNA Complex Is Determined from Gyrase Concentration Dependence of Transcription Elongation Rates

Gyrase-DNA binding can be described by two steps (Gore et al., 2006). First, DNA and gyrase form a complex with limited protein-DNA-binding interface, which is prone to rapid dissociation. Second, a chiral DNA wrap is formed around gyrase, which in the presence of ATP generates negative DNA supercoils. Here, we discuss the binding stability and kinetics of the DNA wrapping state, which are relevant to transcription dynamics.

By titrating the elongation rate on the multiple-biotin template with gyrase (Figure 3C), we determined the gyrase-DNA dissociation constant K_d from the gyrase concentration at which the increase of the T7 transcription elongation rate reaches half of its saturation value, that is $K_d \approx 100$ nM (Extended Experimental Procedures). This K_d is larger than previously reported 0.2∼0.5 nM (Higgins and Cozzarelli, 1982; Maxwell and Gellert, 1984), where specific gyrase-binding sequences were used (Morrison and Cozzarelli, 1981; Rau et al., 1987). Strong gyrase-binding sites comparable to these sequences are sparsely distributed on the *E. coli* chromosome with a frequency of only one per 100 kb (Snyder and Drlica, 1979). The *nuoB-N* DNA sequence (∼12 kb) we used in our in vitro assay better represents a chromosomal DNA loop (∼10 kb) that binds to gyrase

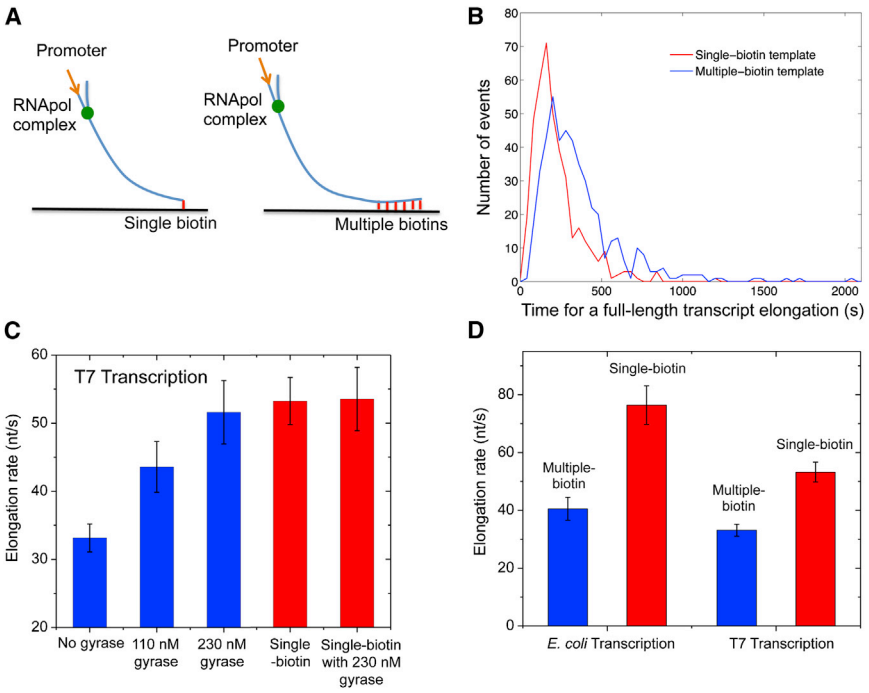

Figure 3. Supercoiling Dependence of Transcription Elongation Rate

(A) In vitro transcription template design containing a T7 or T7A1 promoter and a 12 kb transcribing sequence. The template is anchored to the flow cell surface via either a single or multiple biotin-streptavidin linkages.

(B) Histogram of T7 transcription elongation time on the templates anchored with single (red curve) or multiple biotin-streptavidin linkages (blue curve). The average elongation time for the multiple-biotin template is 60% longer.

(C) Titration of T7 transcription elongation rate (23°C) on the multiple-biotin template (the three bars on the left) with gyrase concentration. The elongation rate increases with the gyrase concentration till it gets as high as that on the single-biotin template (the fourth bar). The elongation rate on the single-biotin template does not change in the presence of a saturating concentration of gyrase (the bar on the right).

(D) *E. coli* transcription elongation rate (37°C) and T7 transcription elongation rate (23°C) on the multiple-biotin template are slower than on the single-biotin template. In (C) and (D), the elongation rates are averaged from over 300 transcripts under each condition. The error bars are bootstrapped confidence intervals (Efron and Tibshirani, 1993).

See also Figures S1 and S2.

at multiple weak binding sites (Franco and Drlica, 1988; Reece and Maxwell, 1991).

Positive Supercoiling Buildup by Transcription Essentially Stops Transcription Initiation

Next, we examined the effect of positive supercoiling on transcription initiation. In order to mimic topologically isolated DNA loops in the bacterial chromosome, we designed a circular template (Figure 4A) and tethered it to the surface with multiple biotin-streptavidin linkages. The circular template consists of a T7 or *E. coli* promoter, a 12-kb-long transcribing sequence, and a T7 or *E. coli* terminator. Due to the low circularization efficiency, a significant fraction of the purified DNAs remained to be linear, which are also tethered on the flow cell surface and transcribed. We picked the circular templates for analysis by staining the DNA molecules with SYTOX Orange and imaging them under flow after recording transcription movies (Figure S3).

For a single template under steady-state condition, transcription initiation rate is the number of initiation events over a fixed period of time (frequency of "spikes" in the intensity trajectory from a template; Figure S4A). According to the ergodic principle, the initiation rate is the sum of initiated events from a population of templates at a specific time point. We measured the total intensity of the circular templates, which is proportional to the initiation rate.

We examined the first steady-state condition, in which T7 transcription occurs on the circular templates in the absence of Topo I and gyrase. A bulky elongation complex generates positive supercoiling ahead of it and negative supercoiling behind it, which annihilate each other when the elongation complex dissociates from the template upon transcription termination (Figure 4A). We found the initiation rate was indeed constant over time because of repetitive annihilation of supercoiling (Figure 4B).

We then examined the second steady-state condition, in which T7 transcription occurs on the circular templates in the presence of both Topo I and gyrase (Figure 4C). Because both positive and negative supercoiling on the DNA template is continuously removed, the initiation rate remained constant over time under this condition (Figure 4D), which is the same as that in the first steady-state condition (Figures S4C and S4D).

We now examine how positive supercoiling buildup would hinder transcription initiation. After introduction of Topo I, negative supercoiling is rapidly removed, and positive supercoiling is expected to accumulate on the circular template as multiple transcripts are made (Figure 4E). Indeed, we observed the initiation rate decreased over time (Figure 4F). Interestingly, the final intensity has dropped to under 20% of its initial value, indicating that transcription initiation was essentially stopped by the buildup of positive supercoiling. This final state corresponds to the gene "off" state. We found that it takes approximately nine rounds of T7 transcription to build up sufficient positive supercoiling that inhibits transcription initiation on a single template in vitro (Figure S4B and Extended Experimental Procedures).

Similar to T7 transcription, we found transcription initiation rate of *E. coli* RNApol dropped to ~25% after approximately five transcripts were produced from a circular template of the same length (12 kb) in the presence of Topo I (Figures 4E, 4G, and S5; Extended Experimental Procedures). We note that fewer than five rounds of transcription might be sufficient to

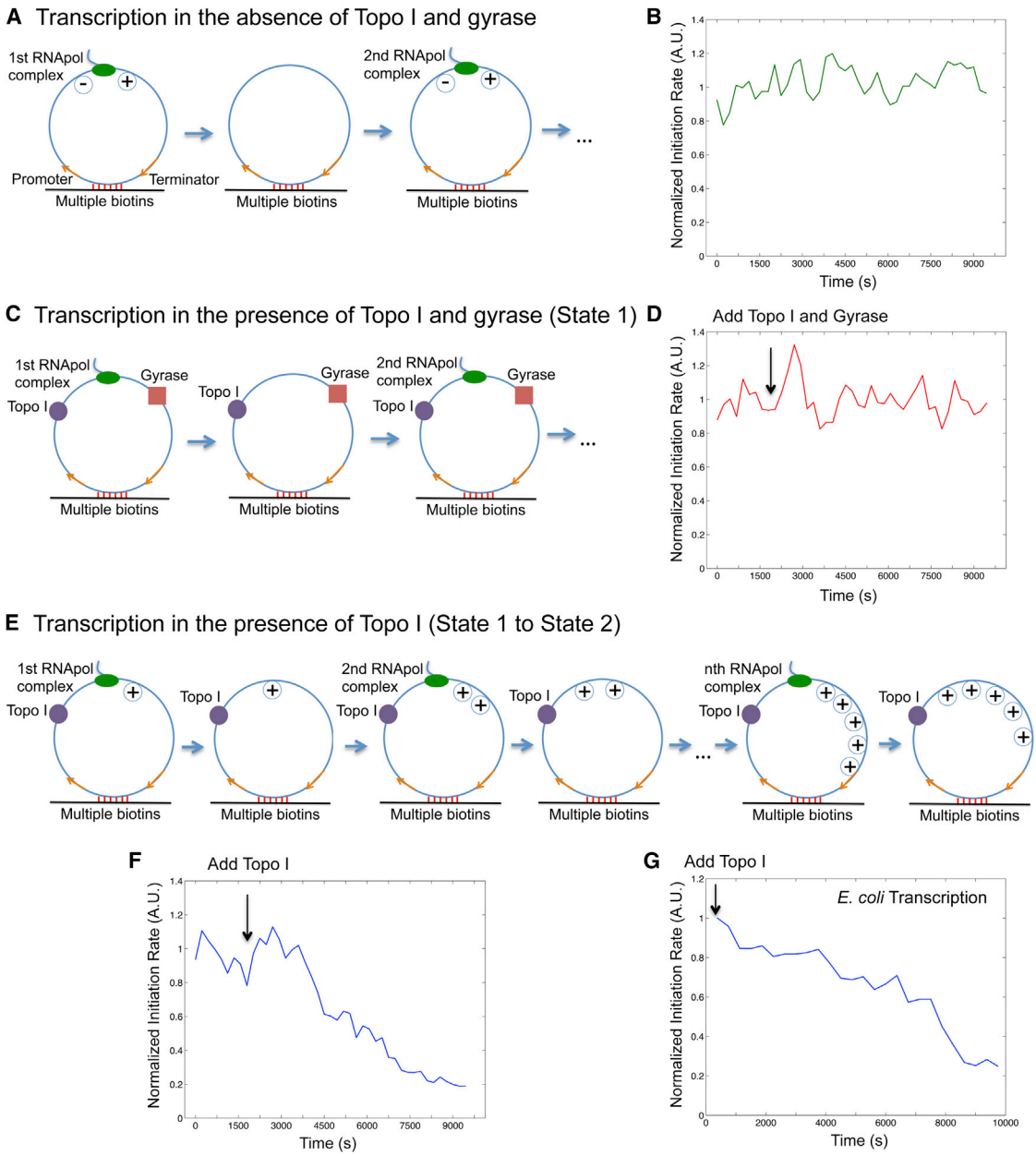

Figure 4. Supercoiling Dependence of Transcription Initiation Rate

(A) Schematic of transcription on a circular template in the absence of topoisomerases. Positive and negative supercoiling annihilate each other after RNApol completes transcription and dissociates from the template.

(B) Time dependence of T7 transcription initiation rate under the condition of (A).

(C) Schematic of transcription on the circular template in the presence of 41 nM Topo I and 0.1 μM gyrase (same as state 1 in Figure 7A).

(D) Time dependence of T7 transcription initiation rate under the condition of (C). The arrow shows the time when the topoisomerases were added into the system.

(E) Schematic of transcription on the circular template in the presence of 41 nM Topo I and absence of gyrase. Positive supercoiling is built up as transcripts are produced.

(F) Time dependence of T7 transcription initiation rate under the condition of (E). (B), (D), and (F) are the total intensity versus time from 160 circular templates under respective conditions normalized to the same fluorescence intensity.

(G) Time dependence of *E. coli* transcription initiation rate in the presence of 62 nM Topo I and absence of gyrase. This is the intensity averaged from 106 circular templates at each time point normalized to that from 209 linear templates (Extended Experimental Procedures).

See also Figures S1, S2, S3, S4, and S5.

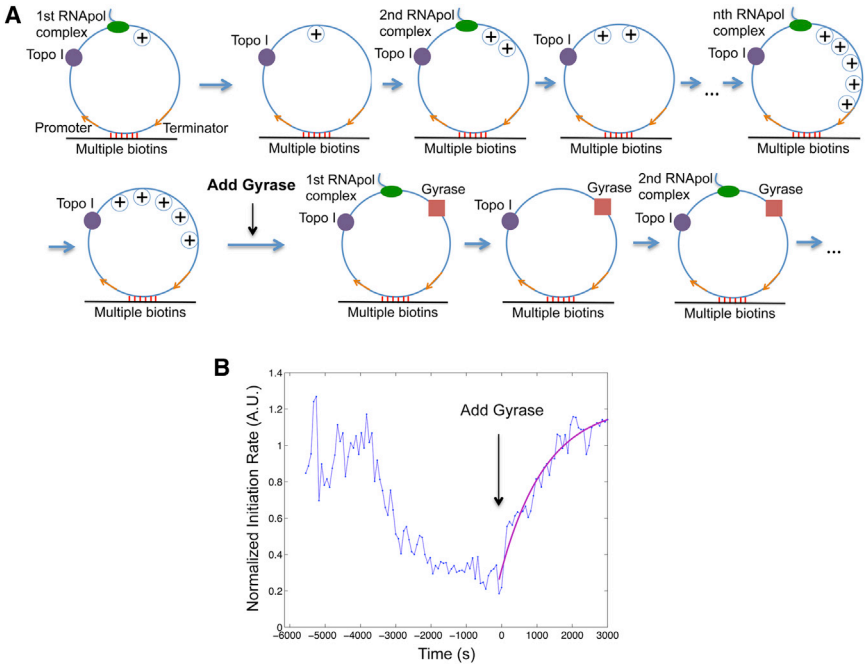

Figure 5. Transition from Gene Off to On State

(A) Schematic of transcription on the circular template first in the presence of 41 nM Topo I only (same as Figure 4E) and then both 41 nM Topo I and 0.1 μM gyrase (same as Figure 4C).

(B) Time dependence of T7 transcription initiation rate (blue) under the condition of (A). This is the intensity averaged from 160 circular templates at each time point normalized to that from 120 linear templates. Gyrase was added into the system at T = 0, when transcription initiation was essentially stopped by positive supercoiling accumulation. The trajectory after T = 0 is fitted with a single exponential function (magenta).

See also Figures S1, S2, and S3.

generate the same level of supercoiling in a live cell, where the environment is more viscous and the elongation complex is bulkier due to transcription-translation coupling (Lynch and Wang, 1993).

With regards to why supercoiling stops transcription initiation, earlier magnetic tweezer experiments have shown that DNA positive supercoiling leads to significantly slower and less stable formation of *E. coli* RNApol-promoter open complex (Revyakin et al., 2004). Therefore, we conclude that the observed inhibition of transcription initiation arises from hindered formation of RNApol-promoter open complex due to positive supercoiling accumulation.

Gyrase Binding to Positively Supercoiled DNA Restarts Transcription

We now prove that gyrase binding on the positively supercoiled DNA restarts transcription. We started with T7 transcription on the circular templates in the presence of Topo I, generating the gene off state (Figure 5). Upon addition of gyrase into the system, transcription initiation rate started to increase and reached a plateau at the initial value of the relaxed templates (Figure 5B), indicating that transcription initiation was fully recovered when positive supercoiling was released by gyrase.

The initiation rate versus time after the introduction of gyrase can be fitted well with a single exponential rise (Figure 5B), suggesting a single step is rate limiting for the transition. The rate constant is determined to be 0.78×10^{-3} s^{-1}, comparable to the pseudo-first-order gyrase-DNA binding rate constant $\sim 10^{-3}$ s^{-1}, which is the product between the bimolecular binding rate constant $k_{on} \approx 10^4$ M^{-1} s^{-1} under our salt concentration (Higgins and Cozzarelli, 1982) and the gyrase concentration used in our in vitro assay 0.1 μM. Such consistency suggests that gyrase binding to the DNA template is the rate-limiting step to restart transcription in vitro.

The K_d and k_{on} of gyrase-DNA binding determined in vitro allow us to estimate the time it takes gyrase to dissociate from and rebind to a specific chromosomal DNA loop in an *E. coli* cell. Because there are comparable numbers of gyrase molecules and chromosomal DNA loops per *E. coli* cell, many gyrase molecules are trapped on DNA loops. According to K_d, the intracellular concentration of unbound gyrase [G] is ~0.3 μM (Extended Experimental Procedures). Because k_{on} of gyrase-DNA binding is $\sim 10^4$ M^{-1} s^{-1} as determined in vitro, the in vivo pseudo-first-order rate constant for gyrase-DNA binding $k_{on} \cdot [G]$ is $\sim 3 \times 10^{-3}$ s^{-1}. Therefore, the average gyrase rebinding time is $1/(k_{on} \cdot [G]) \approx 6$ min. Because the dissociation rate constant of gyrase-DNA complex is $k_{off} = K_d \cdot k_{on} \approx 10^{-3}$ s^{-1}, the average gyrase dissociation time is $1/k_{off} \approx 17$ min. The gyrase rebinding and dissociation time is in the same order of magnitude with the off and on periods of transcriptional bursting observed in live *E. coli* cells (Golding et al., 2005).

In summary, the in vitro experiments demonstrated that DNA positive supercoiling generated by transcription slows down both transcription initiation and elongation and eventually stops initiation. Inhibited transcription initiation and elongation can be recovered upon gyrase binding to DNA. Therefore, accumulation and removal of positive supercoiling of a chromosomal DNA loop containing a highly expressed gene can switch the gene off and on. Next, we performed live-cell experiments to further support this mechanism.

Live-Cell Experiments Confirm that Positive Supercoiling Buildup Slows Down Transcription Elongation

We examined whether chromosomal supercoiling level affects transcription elongation in live *E. coli* cells. Using quantitative RT-PCR, we measured the steady-state abundance of different segments of fully induced *lac* operon mRNA under gyrase

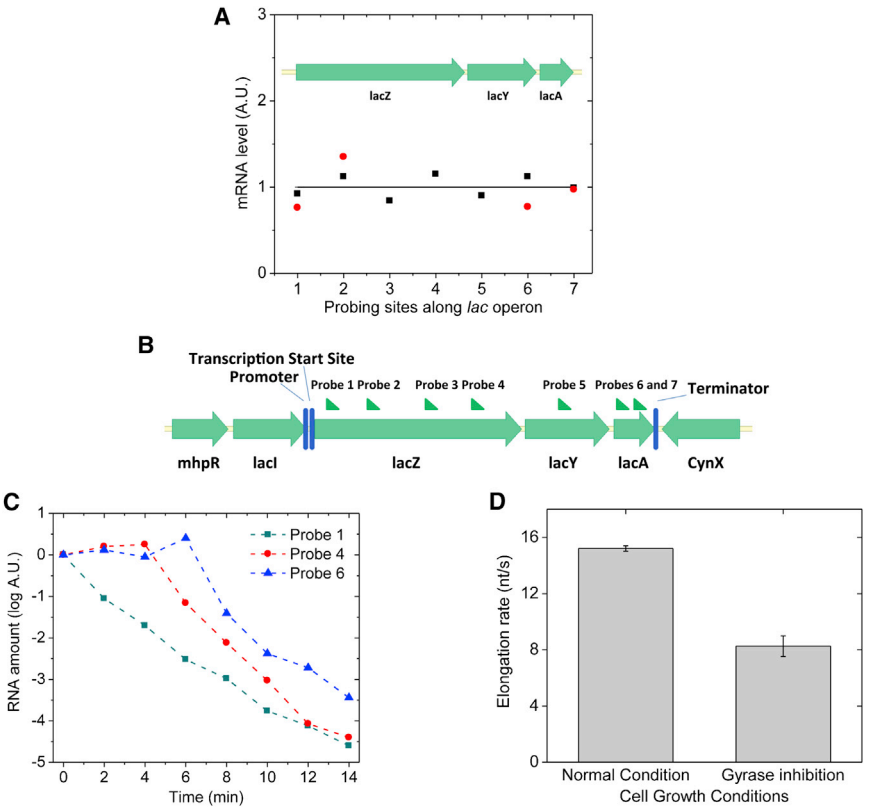

Figure 6. Transcription Processivity and Elongation Rate upon Gyrase Inhibition in Live *E. coli* Cells

(A) Quantitative RT-PCR measurement of the abundance of different parts of *lac* operon mRNA under fully induced condition. x axis: the position of probing sites along *lac* operon; y axis: mRNA abundance. Black squares: gyrase partial inhibition by 50 ng/μl novobiocin; red dots: gyrase complete inhibition by 10 ng/μl norfloxacin. The result indicates nonstop transcription elongation upon positive supercoiling buildup on the DNA. The abundance of each mRNA part is normalized to its abundance under wild-type condition, which is plotted as the flat curve.

(B) Seven sites on *lac* operon mRNA that were probed in the measurement of transcription elongation rate.

(C) Five hundred nanograms per microliter rifampicin was added into the cell culture at time zero to stop transcription initiation, but not elongation. The abundance of different positions on the *lac* operon mRNA was probed by quantitative RT-PCR at multiple time points.

(D) Transcription elongation rate decreased upon gyrase inhibition by 10 ng/μl norfloxacin in live *E. coli* cells. The error bars are SDs of the elongation rates obtained by repeating the measurements (n = 3) under each condition.

See also Figure S6.

inhibition by novobiocin or norfloxacin. No difference in the abundance was observed throughout the transcript (Figure 6A). This result suggests that the elongation complex does not stop or dissociate from the DNA template in the middle of one round of transcription more often when the DNA template is more positively supercoiled. We note that an early in vitro experiment found that stable norfloxacin-gyrase-DNA complex could form at a strong gyrase-binding site and block transcription elongation (Willmott et al., 1994). This effect was not observed in our live-cell assay, likely due to a low intracellular norfloxacin concentration and the lack of strong gyrase-binding sites in the probed region.

Next, we measured transcription elongation rate in live *E. coli* cells using transcription initiation inhibitor rifampicin (Epshtein and Nudler, 2003) and quantitative RT-PCR (H. Chen, K. Shiroguchi, H.G., and X.S.X., unpublished data). We added rifampicin to the cell culture at time zero and measured the mRNA abundance in multiple regions (Figure 6B) along the transcript at multiple time points afterward. Whereas the mRNA abundance at the 5′ end decreased immediately upon the addition of rifampicin, the mRNA abundance downstream started to decrease after a time delay (Figure 6C). The distance between the two probes on the transcript divided by the time delay was the elongation rate. Gyrase inhibition was achieved by norfloxacin treatment where most cells were viable through the 14-min-long rifampicin assay (Figure S6A). We found that the elongation rate of fully induced *lac* operon decreased by 46% upon gyrase inhibition (Figure 6D), similar to the result previously reported by Higgins group on *Salmonella enterica* (Rovinskiy et al., 2012).

A Two-State Model Describes Transcriptional Bursting

Transcriptional bursting has been described with a two-state model, but the origin of the two states was not understood (Golding et al., 2005; Munsky et al., 2012; So et al., 2011). We now understand the mechanism of bacterial transcriptional bursting (Figure 7A): the gene stochastically switches between on and off states due to release and accumulation of positive supercoiling. The on state (state 1) generates mRNAs with an average transcription rate k_1, and the mRNAs degrade with rate constant γ. The off state (state 2) does not generate any mRNA. The interconversion rate constants between the two states are α and β. α is the gene on-to-off transition rate constant due to gyrase dissociation from the DNA loop and positive supercoiling accumulation. For simplicity, we assume positive supercoiling accumulation is fast and gyrase dissociation is rate limiting. β corresponds to the pseudo-first-order rate constant of gyrase-DNA binding, which is also rate limiting in the gene off-to-on transition and proportional to the effective intracellular gyrase concentration. The lower the effective gyrase concentration is, the longer the gene stays in the off state and the smaller the on/off duty cycle ratio (β/α), which should result in a higher extent of bursting reflected by a larger Fano factor and a larger fraction of cells that contain zero copy of mRNA at a given time point.

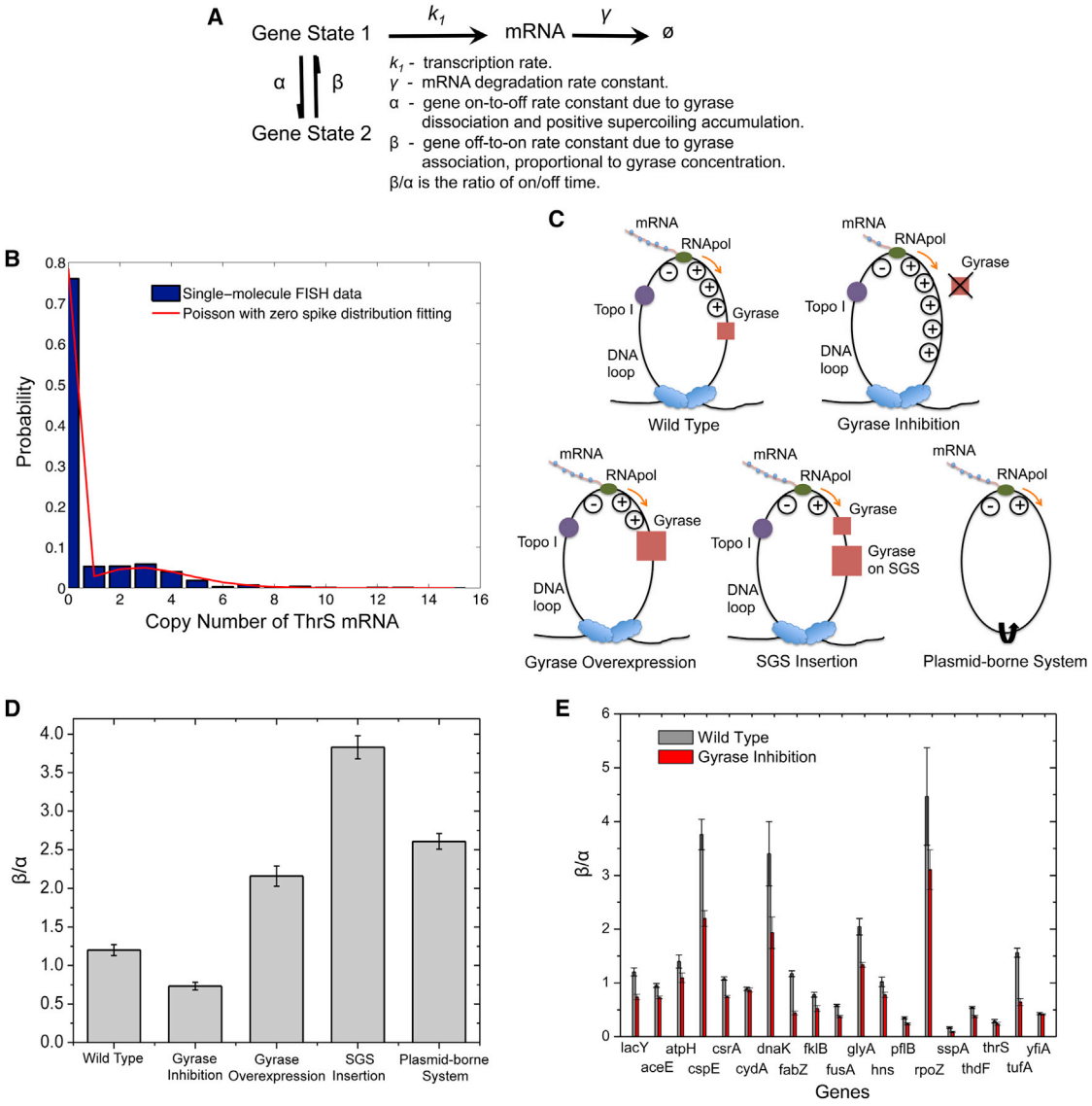

Figure 7. Dependence of On/Off Duty Cycle Ratio, β/α, on Effective Intracellular Gyrase Concentration

(A) Kinetic scheme of the two-state model with relevant rate constants.

(B) Fitting of cellular ThrS mRNA copy number distribution with Poisson with zero spike distribution.

(C) Schematics of interactions between effective gyrase concentration and DNA supercoiling generated by transcription under different conditions. Upon gyrase inhibition, positive supercoiling accumulates on the chromosomal DNA loop to a higher extent than wild-type. Gyrase overexpression or SGS insertion is the opposite. In a plasmid-borne expression module, positive and negative supercoiling annihilate each other due to the lack of topological barriers.

(D) β/α of fully induced *lac* operon decreases upon gyrase partial inhibition by 50 ng/μl novobiocin treatment and increases upon gyrase overexpression, SGS insertion, and in a plasmid-borne system.

(E) β/α of fully induced *lac* operon and other 18 highly transcribed *E. coli* genes. β/α of all the 19 genes decrease upon gyrase partial inhibition by 50 ng/μl novobiocin treatment. In (D) and (E), the error bars are bootstrapped confidence intervals.

See also Figures S6, S7, and Table S1.

Transcription bursts of highly transcribed genes are reflected by the non-Poissonian mRNA copy number distribution. Under the condition that α and β are significantly smaller than k_1 and γ as previously observed (Golding et al., 2005), the steady-state mRNA copy number distribution for a population of cells is bimodal (Munsky et al., 2012) and can be approximated with a "Poisson with zero spike" distribution (Equation 1). Based on the two-state model, the Fano factor (F) can be derived as Equation 2 (Extended Experimental Procedures).

$$p(0) = \frac{\beta}{\alpha+\beta} e^{-\frac{k_1}{\gamma}} + \frac{\alpha}{\alpha+\beta}$$
$$p(n) = \frac{\beta}{\alpha+\beta} e^{-\frac{k_1}{\gamma}} \frac{\left(\frac{k_1}{\gamma}\right)^n}{n!}, n \geq 1. \quad \text{(Equation 1)}$$

$$F = 1 + \frac{\alpha k_1}{(\alpha+\beta)\gamma}. \quad \text{(Equation 2)}$$

We note these results hold only under the condition that gyrase dissociation and rebinding are rate limiting, longer than the time scales of positive supercoiling accumulation and release. Although this is a simplified model, it captures the origin of transcriptional bursting, i.e., gyrase dissociation, and establishes the gyrase concentration dependence of β, which can now be subject to in vivo experimental tests.

The Dependence of Transcriptional Bursting on Effective Gyrase Concentration Revealed by Single-Molecule mRNA FISH Assay

We now experimentally verify this model by measuring the steady-state mRNA copy number distribution in a population of isogenic *E. coli* cells under gyrase inhibition and overexpression conditions. We performed mRNA FISH assay with single-molecule sensitivity, using a single Atto 594-labeled 20-oligomer nucleotide probing the *yfp* sequence in an *E. coli* strain with the target gene fused to *yfp* sequence endogenously. By measuring the intensity of each fluorescent spot and counting the number of spots per cell, we determined cellular mRNA copy number for thousands of *E. coli* cells. The efficiency of our single-molecule mRNA FISH assay is ~90% (Taniguchi et al., 2010).

We measured the cellular mRNA copy number distribution of the fully induced *lac* operon and 18 highly transcribed genes from the YFP library that our group has constructed (Taniguchi et al., 2010). Partial gyrase inhibition was achieved by novobiocin treatment at low concentration without affecting normal bacterial growth and morphology (Figure S6B). We found that the cellular mRNA copy number distribution can be fitted well by the Poisson with zero spike distribution for the 19 genes with excellent coefficients of determination (Figure 7B; Table S1). The fitting allows estimation of the on/off duty cycle ratio of transcriptional bursting (β/α), with an error bar obtained by the bootstrapping method (Efron and Tibshirani, 1993).

For fully induced *lac* operon, β/α was 1.20 for wild-type, decreased to 0.73 upon gyrase inhibition, increased to 2.16 upon gyrase overexpression, and increased to 3.83 when a strong gyrase site (SGS) was inserted next to the *lac* operon (Figures 7C and 7D). This result indicates that transcriptional bursting is sensitively dependent on the availability of gyrase to remove positive supercoiling accumulated during active transcription.

If *lac* operon is on a plasmid that lacks topological constraint, positive and negative supercoiling generated by transcription could diffuse along the circular DNA in opposite directions and annihilate each other (Figure 7C). As a critical control, a plasmid-borne system in *E. coli* indeed showed an even higher β/α than that of gyrase overexpression (Figure 7D).

One would expect β/α to be infinitely large if the gene is always on in the complete absence of positive supercoiling accumulation. Yet it was not the case for the plasmid-borne system because there could be weak and transient topological barriers on the plasmid DNA due to transient protein binding (Leng et al., 2011). To confirm this point, we performed control experiments on the same plasmid-borne system under gyrase inhibition and overexpression conditions. We found that β/α changed in the same direction as the chromosomal gene but to a smaller extent. Under the same conditions, β/α of the plasmid-borne system was always higher than the chromosomal counterpart, because the plasmid has much lower topological barriers and thus more efficient removal of positive supercoiling during active transcription (Figure S6C).

Intriguingly, similar to the scenario of fully induced *lac* operon, all the other 18 genes showed a decreased β/α (Figure 7E) upon gyrase inhibition. In addition, most of the genes showed an increased Fano factor (Figure S7A) and an increased fraction of cells containing zero copy of mRNA (Figure S7B) upon gyrase inhibition. These findings are consistent with the prediction based on our model and demonstrate the ubiquitous effect of gyrase concentration on transcriptional bursting.

DISCUSSION

Mechanism of Transcriptional Bursting under Induced Condition Revealed

Pertinent to the fact that there is only one (or two) copy of the gene in a cell, gene expression is stochastic. In recent years, stochastic gene expression has stimulated wide interest (Blake et al., 2003; Elowitz and Leibler, 2000; Elowitz et al., 2002; Ozbudak et al., 2002; Pedraza and Paulsson, 2008). Such stochasticity, or noise, causes phenotypic variability among genetically identical cells and organisms despite identical histories of environmental exposure (Choi et al., 2008; Maamar et al., 2007) and arises from the fact that DNA, mRNA, and gene regulatory proteins can be present and active at only a few copies per cell. Due to the small copy numbers and the fact that stochastic gene expression cannot be synchronized among different cells, quantitative studies of gene expression at the single-cell level necessitate single-molecule sensitivity for mRNA and protein detection.

The stochastic gene expression dynamics of repressed genes have already been well studied and understood to date (Li and Xie, 2011). For highly expressed genes in both prokaryotic and eukaryotic organisms, bursting transcription has been demonstrated by a number of techniques, including single-molecule FISH assay that counts cellular mRNA copy number (Raj et al., 2006, 2010; Taniguchi et al., 2010; Zong et al., 2010), MS2 or PP7 technique that visualizes single mRNA production in real time (Chubb et al., 2006; Golding et al., 2005; Hocine et al., 2013; Larson et al., 2011; Lionnet et al., 2011; Muramoto et al., 2012), and fluorescent protein (Singh et al., 2010) or luciferase (Suter et al., 2011) as gene expression reporter in live cells. Nevertheless, the mechanism of this ubiquitous phenomenon under induced condition is not understood.

We note that the transcriptional bursting phenomenon studied in this paper is different from transcriptional pausing in prokaryotic and eukaryotic cells (Core et al., 2008; Landick, 2006;

Weixlbaumer et al., 2013), which has been studied by recent single-molecule manipulation (Davenport et al., 2000; Herbert et al., 2006; Hodges et al., 2009; Ma et al., 2013; Shundrovsky et al., 2004) and RNA-sequencing experiments (Churchman and Weissman, 2011; Core et al., 2008). Whereas pausing describes intermittent elongation of a transcript, bursting describes discontinuous production of many transcripts over a much longer time scale and involves inhibition of both transcription initiation and elongation.

We have revealed the origin of stochastic transcriptional bursts in bacteria under induced conditions by conducting a series of in vitro and live-cell experiments and demonstrated that reversible switching between different chromosomal supercoiling levels via gyrase dissociation from and rebinding to a DNA loop gives rise to bursting transcription. We note this is a fundamental mechanism pertinent to the chromosome structure and should be applicable to all the highly expressed genes in prokaryotic cells and even eukaryotic cells. However, the situation of eukaryotic cells is more complex than that of bacteria due to more complicated transcription regulation and the existence of nucleosomes (Raser and O'Shea, 2004).

A Role of DNA Supercoiling in Gene Expression Regulation

The interaction between DNA supercoiling and gene expression in bacteria has been investigated for decades. Our knowledge comes primarily from ensemble studies on the relationship between the global DNA supercoiling level and the gene expression level. On one hand, bacterial DNA supercoiling level affects the expression of a few *E. coli* genes called supercoiling-sensitive genes (Peter et al., 2004) as well as transcription elongation rate (Rovinskiy et al., 2012) due to a combined effect of torsional and bending stress sustained by the supercoiled DNA at the transcription site (Lionberger and Meyhöfer, 2010; ten Heggeler-Bordier et al., 1992). On the other hand, local DNA supercoiling level is generated by transcription, according to the "twin-domain model" developed by Wang and Liu groups in late 1980s (Deng et al., 2005; Leng et al., 2011; Lim et al., 2003; Liu and Wang, 1987; Samul and Leng, 2007; Tsao et al., 1989; Wu et al., 1988). Here, we report a role of DNA supercoiling in gene expression regulation that can only be revealed by single-molecule and single-cell approaches: transient DNA supercoiling generated locally during active transcription gives rise to transcriptional bursting, which is a major source of gene expression noise that causes cell-to-cell variability in an isogenic population. Although earlier work proposed DNA supercoiling can be involved in bursting transcription (Mitarai et al., 2008; So et al., 2011), we have experimentally proved that supercoiling dynamics is the primary origin of transcriptional bursting.

In Vitro, Single-Molecule Transcription Assay

In order to investigate the effect of positive supercoiling buildup on transcription elongation and initiation in a clean and controlled fashion, we developed an in vitro, single-molecule assay that could monitor real-time transcription on individual DNA templates. We note our assay is different from other existing in vitro transcription assays using single-molecule manipulation (Abbondanzieri et al., 2005; Bai et al., 2006; Billingsley et al., 2012; Bustamante et al., 2011; Herbert et al., 2008) or single-molecule fluorescence imaging (Chakraborty et al., 2012; Friedman and Gelles, 2012; Kapanidis et al., 2006; Revyakin et al., 2012; Tang et al., 2009; Zhang et al., 2014). Our assay uses RNA staining so that the elongation process on templates with any sequence can be easily monitored for multiple rounds of transcription on each template. This is a high-throughput measurement because hundreds of templates in one field of view can be monitored simultaneously. The assay will be generally useful for studying other questions in transcription, such as pausing and termination kinetics.

Other Possible Mechanisms of Transcriptional Bursting

The current report proves that stochastic changes of supercoiling level in DNA segments due to gyrase dissociation and rebinding is a main mechanism that gives rise to bursting transcription of highly expressed genes in bacteria. However, we note there could be other possible causes of bacterial transcriptional bursting, such as the change of chromosomal looping structure due to the dissociation and rebinding of nucleoid-associated proteins, as well as facilitated transcription reinitiation due to dynamical gene looping, where an operon DNA places its promoter and terminator in spatial proximity (Hebenstreit, 2013). Although they might cause transcription rate fluctuations in addition to the supercoiling effect that we observed, none of these alternative mechanisms have been experimentally proved to switch genes on and off.

EXPERIMENTAL PROCEDURES

In Vitro Single-Molecule Transcription Assay

To measure transcription elongation rates, T7 RNApol (New England Biolabs) or *E. coli* RNApol (Epicentre), NTPs, 250 nM SYTO RNASelect, and an oxygen scavenger system were added to transcription buffer. After infusing the mixture into the flow cell containing immobilized DNA templates, a fluorescent movie was recorded under 488 nm laser excitation at 0.22 W/cm^2. Images were taken every 20 s for 60–80 min, and the acquisition time of each image was 5 s.

To measure transcription initiation rates, the reaction mixture was the same as that for elongation rate measurements except that higher concentrations of RNApol and NTPs were used. The excitation power density was 0.15 W/cm^2. Images were taken every 75 s with 5 s of image acquisition time.

DNA Staining Assay

In order to locate the linear and circular templates in the field of view, 100 nM SYTOX Orange (Life Technologies) in 50 mM Tris-HCl buffer (pH 8.0) was used to stain the immobilized DNAs after transcription movies were recorded. Fluorescent movies were recorded under 532 nm laser excitation with a power density above 4 W/cm^2. The image acquisition time was 0.3 s. The imaging buffer was kept flowing at 8 ml/hr by a syringe pump (PhD 2000; Harvard Apparatus) during the movie recording.

Single-Molecule mRNA FISH Assay

The BW25993 *E. coli* cells were grown in M9 medium with 0.4% glycerol, amino acids, and vitamins, together with antibiotics and saturating amount of isopropyl β-D-thiogalactopyranoside (IPTG) if necessary. The cells were subsequently inoculated 1:500 into the same medium and incubated for ~7 hr at 37°C with 250 rpm shaking till optical density 600 nm (OD_{600nm}) reached 0.2~0.3. Fifty nanograms per microliter novobiocin (Sigma) was added into the medium and incubated for another 2 hr before harvest. Two hours was long enough (several cell cycles) to allow all the cells to enter steady state and thus minimized potential cell-to-cell variation due to different transition kinetics in response to the drug treatment.

The YFP library strains were grown in Luria broth (LB) medium with chloramphenicol at 30°C. The cells were subsequently inoculated 1:400 into M9 medium with 0.4% glucose, amino acids, and vitamins and incubated for 11 hr at 30°C with 250 rpm shaking till OD_{600nm} reached 0.2∼0.3. Fifty nanograms per microliter novobiocin was added and incubated for another 2 hr before harvest.

Single-molecule mRNA FISH assay was performed as previously described (Taniguchi et al., 2010) using Venus495r mRNA FISH probe covalently linked to a dye molecule Atto 594 (Sigma-Aldrich). The images were taken under epi-illumination by a fiber laser at 580 nm and phase contrast illumination by a halogen lamp.

SUPPLEMENTAL INFORMATION

Supplemental Information includes Extended Experimental Procedures, seven figures, and one table and can be found with this article online at http://dx.doi.org/10.1016/j.cell.2014.05.038.

AUTHOR CONTRIBUTIONS

X.S.X. conceived the project and supervised the experiments. S.C. developed the in vitro, single-molecule transcription assay. S.C. performed the in vitro imaging experiments, data analysis, and biophysical calculations based on the in vitro data. S.C. and C.C. performed the control of the enzyme activities in the in vitro, single-molecule transcription assay. C.C. performed the single-molecule mRNA FISH assay, data analysis, and live-cell experiments based on quantitative RT-PCR. C.C. made the DNA constructs for the in vitro, single-molecule assay and the FISH assay. H.G. built the mathematical model. H.G., C.C., and S.C fitted the model to the single-molecule FISH data. S.C., C.C., and X.S.X. designed the experiments and wrote the manuscript.

ACKNOWLEDGMENTS

We thank Xiaowei Zhuang for the collaboration on bacterial chromosomal structure study, which prompted us to conduct the current study; N. Patrick Higgins for providing the plasmid containing strong gyrase site sequence; Gene-Wei Li for development of FISH protocol; Minbiao Ji for help with microscope construction; Rahul Roy for advice on data analysis; and James Wang, Long Cai, Gene-Wei Li, and Paul Choi for critical reading of the manuscript. This work was supported by NIH Pioneer Award (1DP1OD000277; to X.S.X.), NIH grant TR01 (5R01GM096450-02; to X.S.X.), National Science Foundation of China (21373021; to H.G.), and the Foundation for the Author of National Excellent Doctoral Dissertation of China (201119; to H.G.).

Received: September 25, 2013
Revised: March 17, 2014
Accepted: May 8, 2014
Published: July 17, 2014

REFERENCES

Abbondanzieri, E.A., Greenleaf, W.J., Shaevitz, J.W., Landick, R., and Block, S.M. (2005). Direct observation of base-pair stepping by RNA polymerase. Nature *438*, 460–465.

Bai, L., Santangelo, T.J., and Wang, M.D. (2006). Single-molecule analysis of RNA polymerase transcription. Annu. Rev. Biophys. Biomol. Struct. *35*, 343–360.

Baker, T.A., Funnell, B.E., and Kornberg, A. (1987). Helicase action of dnaB protein during replication from the Escherichia coli chromosomal origin in vitro. J. Biol. Chem. *262*, 6877–6885.

Billingsley, D.J., Bonass, W.A., Crampton, N., Kirkham, J., and Thomson, N.H. (2012). Single-molecule studies of DNA transcription using atomic force microscopy. Phys. Biol. *9*, 021001.

Blake, W.J., KAErn, M., Cantor, C.R., and Collins, J.J. (2003). Noise in eukaryotic gene expression. Nature *422*, 633–637.

Efron, B., and Tibshirani, R.J. (1993). An Introduction to the Bootstrap (New York: Chapman & Hall).

Bustamante, C., Cheng, W., and Mejia, Y.X. (2011). Revisiting the central dogma one molecule at a time. Cell *144*, 480–497.

Chakraborty, A., Wang, D., Ebright, Y.W., Korlann, Y., Kortkhonjia, E., Kim, T., Chowdhury, S., Wigneshweraraj, S., Irschik, H., Jansen, R., et al. (2012). Opening and closing of the bacterial RNA polymerase clamp. Science *337*, 591–595.

Cheng, B., Zhu, C.X., Ji, C., Ahumada, A., and Tse-Dinh, Y.C. (2003). Direct interaction between Escherichia coli RNA polymerase and the zinc ribbon domains of DNA topoisomerase I. J. Biol. Chem. *278*, 30705–30710.

Choi, P.J., Cai, L., Frieda, K., and Xie, X.S. (2008). A stochastic single-molecule event triggers phenotype switching of a bacterial cell. Science *322*, 442–446.

Chubb, J.R., Trcek, T., Shenoy, S.M., and Singer, R.H. (2006). Transcriptional pulsing of a developmental gene. Curr. Biol. *16*, 1018–1025.

Churchman, L.S., and Weissman, J.S. (2011). Nascent transcript sequencing visualizes transcription at nucleotide resolution. Nature *469*, 368–373.

Core, L.J., Waterfall, J.J., and Lis, J.T. (2008). Nascent RNA sequencing reveals widespread pausing and divergent initiation at human promoters. Science *322*, 1845–1848.

Davenport, R.J., Wuite, G.J., Landick, R., and Bustamante, C. (2000). Single-molecule study of transcriptional pausing and arrest by E. coli RNA polymerase. Science *287*, 2497–2500.

Deng, S., Stein, R.A., and Higgins, N.P. (2004). Transcription-induced barriers to supercoil diffusion in the Salmonella typhimurium chromosome. Proc. Natl. Acad. Sci. USA *101*, 3398–3403.

Deng, S., Stein, R.A., and Higgins, N.P. (2005). Organization of supercoil domains and their reorganization by transcription. Mol. Microbiol. *57*, 1511–1521.

Drlica, K. (1992). Control of bacterial DNA supercoiling. Mol. Microbiol. *6*, 425–433.

Drolet, M. (2006). Growth inhibition mediated by excess negative supercoiling: the interplay between transcription elongation, R-loop formation and DNA topology. Mol. Microbiol. *59*, 723–730.

El Hanafi, D., and Bossi, L. (2000). Activation and silencing of leu-500 promoter by transcription-induced DNA supercoiling in the Salmonella chromosome. Mol. Microbiol. *37*, 583–594.

Elowitz, M.B., and Leibler, S. (2000). A synthetic oscillatory network of transcriptional regulators. Nature *403*, 335–338.

Elowitz, M.B., Levine, A.J., Siggia, E.D., and Swain, P.S. (2002). Stochastic gene expression in a single cell. Science *297*, 1183–1186.

Epshtein, V., and Nudler, E. (2003). Cooperation between RNA polymerase molecules in transcription elongation. Science *300*, 801–805.

Franco, R.J., and Drlica, K. (1988). DNA gyrase on the bacterial chromosome. Oxolinic acid-induced DNA cleavage in the dnaA-gyrB region. J. Mol. Biol. *201*, 229–233.

Friedman, L.J., and Gelles, J. (2012). Mechanism of transcription initiation at an activator-dependent promoter defined by single-molecule observation. Cell *148*, 679–689.

Golding, I., Paulsson, J., Zawilski, S.M., and Cox, E.C. (2005). Real-time kinetics of gene activity in individual bacteria. Cell *123*, 1025–1036.

Gore, J., Bryant, Z., Stone, M.D., Nöllmann, M., Cozzarelli, N.R., and Bustamante, C. (2006). Mechanochemical analysis of DNA gyrase using rotor bead tracking. Nature *439*, 100–104.

Guptasarma, P. (1996). Cooperative relaxation of supercoils and periodic transcriptional initiation within polymerase batteries. BioEssays *18*, 325–332.

Hardy, C.D., and Cozzarelli, N.R. (2005). A genetic selection for supercoiling mutants of Escherichia coli reveals proteins implicated in chromosome structure. Mol. Microbiol. *57*, 1636–1652.

Hebenstreit, D. (2013). Are gene loops the cause of transcriptional noise? Trends Genet. *29*, 333–338.

Herbert, K.M., La Porta, A., Wong, B.J., Mooney, R.A., Neuman, K.C., Landick, R., and Block, S.M. (2006). Sequence-resolved detection of pausing by single RNA polymerase molecules. Cell *125*, 1083–1094.

Herbert, K.M., Greenleaf, W.J., and Block, S.M. (2008). Single-molecule studies of RNA polymerase: motoring along. Annu. Rev. Biochem. *77*, 149–176.

Higgins, N.P., and Cozzarelli, N.R. (1982). The binding of gyrase to DNA: analysis by retention by nitrocellulose filters. Nucleic Acids Res. *10*, 6833–6847.

Higgins, N.P., Peebles, C.L., Sugino, A., and Cozzarelli, N.R. (1978). Purification of subunits of Escherichia coli DNA gyrase and reconstitution of enzymatic activity. Proc. Natl. Acad. Sci. USA *75*, 1773–1777.

Hocine, S., Raymond, P., Zenklusen, D., Chao, J.A., and Singer, R.H. (2013). Single-molecule analysis of gene expression using two-color RNA labeling in live yeast. Nat. Methods *10*, 119–121.

Hodges, C., Bintu, L., Lubkowska, L., Kashlev, M., and Bustamante, C. (2009). Nucleosomal fluctuations govern the transcription dynamics of RNA polymerase II. Science *325*, 626–628.

Kannemeier, C., Shibamiya, A., Nakazawa, F., Trusheim, H., Ruppert, C., Markart, P., Song, Y., Tzima, E., Kennerknecht, E., Niepmann, M., et al. (2007). Extracellular RNA constitutes a natural procoagulant cofactor in blood coagulation. Proc. Natl. Acad. Sci. USA *104*, 6388–6393.

Kapanidis, A.N., Margeat, E., Ho, S.O., Kortkhonjia, E., Weiss, S., and Ebright, R.H. (2006). Initial transcription by RNA polymerase proceeds through a DNA-scrunching mechanism. Science *314*, 1144–1147.

Kussell, E., and Leibler, S. (2005). Phenotypic diversity, population growth, and information in fluctuating environments. Science *309*, 2075–2078.

Landick, R. (2006). The regulatory roles and mechanism of transcriptional pausing. Biochem. Soc. Trans. *34*, 1062–1066.

Larson, D.R., Zenklusen, D., Wu, B., Chao, J.A., and Singer, R.H. (2011). Real-time observation of transcription initiation and elongation on an endogenous yeast gene. Science *332*, 475–478.

Leng, F., Chen, B., and Dunlap, D.D. (2011). Dividing a supercoiled DNA molecule into two independent topological domains. Proc. Natl. Acad. Sci. USA *108*, 19973–19978.

Li, G.W., and Xie, X.S. (2011). Central dogma at the single-molecule level in living cells. Nature *475*, 308–315.

Lim, H.M., Lewis, D.E., Lee, H.J., Liu, M., and Adhya, S. (2003). Effect of varying the supercoiling of DNA on transcription and its regulation. Biochemistry *42*, 10718–10725.

Lionberger, T.A., and Meyhöfer, E. (2010). Bending the rules of transcriptional repression: tightly looped DNA directly represses T7 RNA polymerase. Biophys. J. *99*, 1139–1148.

Lionnet, T., Czaplinski, K., Darzacq, X., Shav-Tal, Y., Wells, A.L., Chao, J.A., Park, H.Y., de Turris, V., Lopez-Jones, M., and Singer, R.H. (2011). A transgenic mouse for in vivo detection of endogenous labeled mRNA. Nat. Methods *8*, 165–170.

Liu, L.F., and Wang, J.C. (1987). Supercoiling of the DNA template during transcription. Proc. Natl. Acad. Sci. USA *84*, 7024–7027.

Lynch, A.S., and Wang, J.C. (1993). Anchoring of DNA to the bacterial cytoplasmic membrane through cotranscriptional synthesis of polypeptides encoding membrane proteins or proteins for export: a mechanism of plasmid hypernegative supercoiling in mutants deficient in DNA topoisomerase I. J. Bacteriol. *175*, 1645–1655.

Ma, J., Bai, L., and Wang, M.D. (2013). Transcription under torsion. Science *340*, 1580–1583.

Maamar, H., Raj, A., and Dubnau, D. (2007). Noise in gene expression determines cell fate in Bacillus subtilis. Science *317*, 526–529.

Maxwell, A., and Gellert, M. (1984). The DNA dependence of the ATPase activity of DNA gyrase. J. Biol. Chem. *259*, 14472–14480.

Mitarai, N., Dodd, I.B., Crooks, M.T., and Sneppen, K. (2008). The generation of promoter-mediated transcriptional noise in bacteria. PLoS Comput. Biol. *4*, e1000109.

Morrison, A., and Cozzarelli, N.R. (1981). Contacts between DNA gyrase and its binding site on DNA: features of symmetry and asymmetry revealed by protection from nucleases. Proc. Natl. Acad. Sci. USA *78*, 1416–1420.

Munsky, B., Neuert, G., and van Oudenaarden, A. (2012). Using gene expression noise to understand gene regulation. Science *336*, 183–187.

Muramoto, T., Cannon, D., Gierlinski, M., Corrigan, A., Barton, G.J., and Chubb, J.R. (2012). Live imaging of nascent RNA dynamics reveals distinct types of transcriptional pulse regulation. Proc. Natl. Acad. Sci. USA *109*, 7350–7355.

Ozbudak, E.M., Thattai, M., Kurtser, I., Grossman, A.D., and van Oudenaarden, A. (2002). Regulation of noise in the expression of a single gene. Nat. Genet. *31*, 69–73.

Pedraza, J.M., and Paulsson, J. (2008). Effects of molecular memory and bursting on fluctuations in gene expression. Science *319*, 339–343.

Peter, B.J., Arsuaga, J., Breier, A.M., Khodursky, A.B., Brown, P.O., and Cozzarelli, N.R. (2004). Genomic transcriptional response to loss of chromosomal supercoiling in Escherichia coli. Genome Biol. *5*, R87.

Postow, L., Hardy, C.D., Arsuaga, J., and Cozzarelli, N.R. (2004). Topological domain structure of the Escherichia coli chromosome. Genes Dev. *18*, 1766–1779.

Raj, A., Peskin, C.S., Tranchina, D., Vargas, D.Y., and Tyagi, S. (2006). Stochastic mRNA synthesis in mammalian cells. PLoS Biol. *4*, e309.

Raj, A., Rifkin, S.A., Andersen, E., and van Oudenaarden, A. (2010). Variability in gene expression underlies incomplete penetrance. Nature *463*, 913–918.

Raser, J.M., and O'Shea, E.K. (2004). Control of stochasticity in eukaryotic gene expression. Science *304*, 1811–1814.

Rau, D.C., Gellert, M., Thoma, F., and Maxwell, A. (1987). Structure of the DNA gyrase-DNA complex as revealed by transient electric dichroism. J. Mol. Biol. *193*, 555–569.

Reece, R.J., and Maxwell, A. (1991). DNA gyrase: structure and function. Crit. Rev. Biochem. Mol. Biol. *26*, 335–375.

Revyakin, A., Ebright, R.H., and Strick, T.R. (2004). Promoter unwinding and promoter clearance by RNA polymerase: detection by single-molecule DNA nanomanipulation. Proc. Natl. Acad. Sci. USA *101*, 4776–4780.

Revyakin, A., Zhang, Z., Coleman, R.A., Li, Y., Inouye, C., Lucas, J.K., Park, S.R., Chu, S., and Tjian, R. (2012). Transcription initiation by human RNA polymerase II visualized at single-molecule resolution. Genes Dev. *26*, 1691–1702.

Rovinskiy, N., Agbleke, A.A., Chesnokova, O., Pang, Z., and Higgins, N.P. (2012). Rates of gyrase supercoiling and transcription elongation control supercoil density in a bacterial chromosome. PLoS Genet. *8*, e1002845.

Samul, R., and Leng, F. (2007). Transcription-coupled hypernegative supercoiling of plasmid DNA by T7 RNA polymerase in Escherichia coli topoisomerase I-deficient strains. J. Mol. Biol. *374*, 925–935.

Shundrovsky, A., Santangelo, T.J., Roberts, J.W., and Wang, M.D. (2004). A single-molecule technique to study sequence-dependent transcription pausing. Biophys. J. *87*, 3945–3953.

Singh, A., Razooky, B., Cox, C.D., Simpson, M.L., and Weinberger, L.S. (2010). Transcriptional bursting from the HIV-1 promoter is a significant source of stochastic noise in HIV-1 gene expression. Biophys. J. *98*, L32–L34.

Skinner, G.M., Baumann, C.G., Quinn, D.M., Molloy, J.E., and Hoggett, J.G. (2004). Promoter binding, initiation, and elongation by bacteriophage T7 RNA polymerase. A single-molecule view of the transcription cycle. J. Biol. Chem. *279*, 3239–3244.

Snyder, M., and Drlica, K. (1979). DNA gyrase on the bacterial chromosome: DNA cleavage induced by oxolinic acid. J. Mol. Biol. *131*, 287–302.

So, L.H., Ghosh, A., Zong, C., Sepúlveda, L.A., Segev, R., and Golding, I. (2011). General properties of transcriptional time series in Escherichia coli. Nat. Genet. *43*, 554–560.

Suter, D.M., Molina, N., Gatfield, D., Schneider, K., Schibler, U., and Naef, F. (2011). Mammalian genes are transcribed with widely different bursting kinetics. Science *332*, 472–474.

Tang, G.Q., Roy, R., Bandwar, R.P., Ha, T., and Patel, S.S. (2009). Real-time observation of the transition from transcription initiation to elongation of the RNA polymerase. Proc. Natl. Acad. Sci. USA *106*, 22175–22180.

Taniguchi, Y., Choi, P.J., Li, G.W., Chen, H., Babu, M., Hearn, J., Emili, A., and Xie, X.S. (2010). Quantifying E. coli proteome and transcriptome with single-molecule sensitivity in single cells. Science *329*, 533–538.

ten Heggeler-Bordier, B., Wahli, W., Adrian, M., Stasiak, A., and Dubochet, J. (1992). The apical localization of transcribing RNA polymerases on supercoiled DNA prevents their rotation around the template. EMBO J. *11*, 667–672.

Thattai, M., and van Oudenaarden, A. (2004). Stochastic gene expression in fluctuating environments. Genetics *167*, 523–530.

Tsao, Y.P., Wu, H.Y., and Liu, L.F. (1989). Transcription-driven supercoiling of DNA: direct biochemical evidence from in vitro studies. Cell *56*, 111–118.

Wang, W., Li, G.W., Chen, C., Xie, X.S., and Zhuang, X. (2011). Chromosome organization by a nucleoid-associated protein in live bacteria. Science *333*, 1445–1449.

Weixlbaumer, A., Leon, K., Landick, R., and Darst, S.A. (2013). Structural basis of transcriptional pausing in bacteria. Cell *152*, 431–441.

Willmott, C.J., Critchlow, S.E., Eperon, I.C., and Maxwell, A. (1994). The complex of DNA gyrase and quinolone drugs with DNA forms a barrier to transcription by RNA polymerase. J. Mol. Biol. *242*, 351–363.

Wolf, D.M., Vazirani, V.V., and Arkin, A.P. (2005). Diversity in times of adversity: probabilistic strategies in microbial survival games. J. Theor. Biol. *234*, 227–253.

Wu, H.Y., Shyy, S.H., Wang, J.C., and Liu, L.F. (1988). Transcription generates positively and negatively supercoiled domains in the template. Cell *53*, 433–440.

Zhang, Z., Revyakin, A., Grimm, J.B., Lavis, L.D., and Tjian, R. (2014). Single-molecule tracking of the transcription cycle by sub-second RNA detection. eLife *3*, e01775.

Zong, C., So, L.H., Sepúlveda, L.A., Skinner, S.O., and Golding, I. (2010). Lysogen stability is determined by the frequency of activity bursts from the fate-determining gene. Mol. Syst. Biol. *6*, 440.